

Multi-period Co-optimization of Transmission and Wind Turbine Generation Expansion Planning with Short-circuit Constraints Under Deregulated Environment

Zhaoqin Hu, Yunpeng Xiao, *Senior Member, IEEE*, Xiuli Wang, *Senior Member, IEEE*, and Xifan Wang, *Life Fellow, IEEE*

Abstract—The increase in the penetration rate of renewable energy exacerbates the rise in system short-circuit level. Thus, short-circuit constraints (SCCs) are crucial in the co-optimization of transmission and generation expansion planning. The deregulated environment further complicates this process by assigning responsibilities for transmission and generation to separate market entities. This paper proposes a multi-period co-optimization method of transmission and wind turbine generation expansion planning to address this challenge. The transmission expansion planning (TEP) problem limits the short-circuit level, which could be elevated by lines, synchronous generators, and wind turbine generators. The method is formulated as a tri-level mixed-integer linear programming (MILP) problem, where an equilibrium problem with equilibrium constraints is formed at the second and third levels. This problem is restructured into a MILP problem with Nash equilibrium conditions via complementarity problem reformulation. We propose an iterative algorithm targeting the SCCs to solve it. The effectiveness of the proposed method is validated on the IEEE 24-bus reliability test system through comparisons with three existing TEP methods, analyzing the impact of SCCs and generation expansion planning on TEP and the system operating cost under a deregulated environment.

Index Terms—Co-optimization, generation expansion planning, transmission expansion planning (TEP), wind turbine, electricity market, short-circuit constraint.

NOMENCLATURE

A. Indices

\wedge	Superscript of variables under specific decisions
τ	Index of scenarios
bus(\cdot)	Superscript of node where generator is located

f	Superscript of short-circuit current
fr(\cdot), to(\cdot)	Superscripts of starting and ending nodes of line
g, r	Indices of generators
i, j, m, n	Indices of buses
k	Superscript of iteration times
l	Index of lines
s_g	Index of decisions
t	Index of years
F	Index of faulty buses

B. Sets

Ω_τ	Index set of scenarios
\mathcal{C}	Index set of generators
\mathcal{C}^W	Index set of wind turbine generators
\mathcal{C}_{candi}^G	Index set of candidate synchronous generators
\mathcal{C}_{exist}^G	Index set of existing synchronous generators
\mathcal{C}_{candi}^W	Index set of candidate wind turbine generators
\mathcal{H}^k	Index set of $u_{g,t}^*$
\mathcal{L}	Index set of transmission lines
\mathcal{L}_{candi}	Index set of candidate transmission lines
\mathcal{L}_{exist}	Index set of existing transmission lines
\mathcal{N}	Index set of buses
\mathcal{S}_g	Index set of decisions for generator g
\mathcal{T}	Index set of years
\mathcal{U}^k	Index set of Nash equilibrium (NE) solution
\mathcal{V}^k	Index set of transmission expansion planning (TEP) solution $v_{l,t}^k$
\mathcal{W}^k	Index set of TEP solution $w_{l,t}^k$

C. Constants

α_τ	Renewable output fluctuation in scenario τ
μ_τ	Load demand fluctuation in scenario τ
Γ_τ	Equivalent hour in scenario τ
C_n^{Eq}	Annualized investment coefficient

Manuscript received: March 19, 2025; revised: May 10, 2025; accepted: July 8, 2025. Date of CrossCheck: July 8, 2025. Date of online publication: July 28, 2025.

This work was supported by National Natural Science Foundation of China (No. 52307136).

This article is distributed under the terms of the Creative Commons Attribution 4.0 International License (<http://creativecommons.org/licenses/by/4.0/>).

Z. Hu, Y. Xiao (corresponding author), X. Wang, and X. Wang are with the School of Electrical Engineering, Xi'an Jiaotong University, Xi'an 710049, China (e-mail: zqhi@stu.xjtu.edu.cn; ypxiao@xjtu.edu.cn; xiuliw@xjtu.edu.cn; xfwang@mail.xjtu.edu.cn).

DOI: 10.35833/MPCE.2025.000233



$D_{i,t}$	Load demand at bus i in year t
I_r^N	Nominal current of generator r
I_i^0	Injected current at bus i before fault
I_F^{Sc}	Interrupting rating of circuit breaker at fault bus F
I_r^f	Fixed current of generator r during fault
I_F^f	Short-circuit current at faulty bus F
ΔI_F^f	Fault current component at faulty bus F
IC_g^G, IC_l^L	Investment costs of generator g and line l
LCM_t	Allowed new line capacity in year t
LFM_t	Allowed new line cost in year t
$LN M_t$	Allowed new line number in year t
M	A large value
M^θ	Penalty for loss of load
M^ε	Penalty for short-circuit level over limit
MI, MD_l	The minimum durations of offline and online states of line l
\bar{P}_g^G	Upper bound for $p_{g,\tau,t}^g$
\bar{P}_l^f	Power flow capacity of line l
PC_g^G	Operating cost of generator g
PC^θ	The maximum price
SNM_t	The maximum number of lines available for switching operations in year t
T^{\max}	Construction time
U_F^0	Voltage at fault bus F before fault
ΔU_F	Fault voltage component at fault bus F
$X_{ii}, \Delta X_{ii}$	The i^{th} -row and i^{th} -column element of reactance matrix and its change value
X_{ii}^0	Value of X_{ii} before fault
$\Delta X_g, \Delta X_l$	Change values of reactance from generator g and line l
Z_{ii}	The i^{th} -row and i^{th} -column element of impedance matrix

D. Variables

$\theta_{i,\tau,t}$	Phase angle at bus i in scenario τ in year t
$\Theta_{i,\tau,t}$	Loss of load at bus i in scenario τ in year t
$\Xi_{i,t}$	Short-circuit level over limit at bus i in year t
$a^{(x)}$	Auxiliary variable introduced for dual variable x
Gpr_g^G	Profit from expansion of generator g
$p_{l,\tau,t}^f$	Power flow of line l in scenario τ in year t
$p_{g,\tau,t}^g$	Output of generator g in scenario τ in year t
$u_{g,t}$	Binary variable that is equal to 1 if generator g is built in year t , and 0 otherwise
$u_{g,t}^s$	Specific decision of $u_{g,t}$
$v_{l,t}$	Binary variable that is equal to 1 if line l is built in year t , and 0 otherwise
$w_{l,t}$	Binary variable that is equal to 1 if line l is on-line in year t , and 0 otherwise
$y_{l,t}$	Binary variable that is equal to 1 if line l is switched on in year t , and 0 otherwise

$z_{l,t}$	Binary variable that is equal to 1 if line l is switched off in year t , and 0 otherwise
-----------	--

E. Dual Variables

$\gamma_{g,\tau,t}^{\text{lo}}, \gamma_{g,\tau,t}^{\text{up}}$	Dual variables of left and right inequality constraints of (29)
$\zeta_{ri,\tau,t}^{\text{lo}}, \zeta_{ri,\tau,t}^{\text{up}}$	Dual variables of left and right inequality constraints of (31)
$\lambda_{i,\tau,t}$	Dual variable of equality constraint (24)
$\nu_{l,\tau,t}^{\text{lo}}, \nu_{l,\tau,t}^{\text{up}}$	Dual variables of left and right inequality constraints of (25)
$\xi_{g,\tau,t}^{\text{lo}}, \xi_{g,\tau,t}^{\text{up}}$	Dual variables of left and right inequality constraints of (30)
$\pi_{l,\tau,t}^{\text{lo}}, \pi_{l,\tau,t}^{\text{up}}$	Dual variables of left and right inequality constraints of (26)
$\phi_{l,\tau,t}^{\text{lo}}, \phi_{l,\tau,t}^{\text{up}}$	Dual variables of left and right inequality constraints of (27)
$\psi_{l,\tau,t}^{\text{lo}}, \psi_{l,\tau,t}^{\text{up}}$	Dual variables of left and right inequality constraints of (28)
$\omega_{i,\tau,t}$	Dual variable of inequality constraint (32)

F. Auxiliary Variables

$a_{g,\tau,t}^{\zeta^{\text{lo}}}, a_{g,\tau,t}^{\zeta^{\text{up}}}$	Auxiliary variables representing product of $u_{g,t}$ with $\zeta_{g,\tau,t}^{\text{lo}}$ and $\zeta_{g,\tau,t}^{\text{up}}$
$a_{l,\tau,t}^{\nu^{\text{lo}}}, a_{l,\tau,t}^{\nu^{\text{up}}}$	Auxiliary variables representing product of $w_{l,t}$ with $\nu_{l,\tau,t}^{\text{lo}}$ and $\nu_{l,\tau,t}^{\text{up}}$
$a_{g,\tau,t}^{\xi^{\text{lo}}}, a_{g,\tau,t}^{\xi^{\text{up}}}$	Auxiliary variables representing product of $u_{g,t}$ with $\xi_{g,\tau,t}^{\text{lo}}$ and $\xi_{g,\tau,t}^{\text{up}}$
$a_{l,\tau,t}^{\pi^{\text{lo}}}, a_{l,\tau,t}^{\pi^{\text{up}}}$	Auxiliary variables representing product of $v_{l,t}$ with $\pi_{l,\tau,t}^{\text{lo}}$ and $\pi_{l,\tau,t}^{\text{up}}$
$a_{l,\tau,t}^{\phi^{\text{lo}}}, a_{l,\tau,t}^{\phi^{\text{up}}}$	Auxiliary variables representing product of $w_{l,t}$ with $\phi_{l,\tau,t}^{\text{lo}}$ and $\phi_{l,\tau,t}^{\text{up}}$
$a_{l,\tau,t}^{\psi^{\text{lo}}}, a_{l,\tau,t}^{\psi^{\text{up}}}$	Auxiliary variables representing product of $v_{l,t}$ with $\psi_{l,\tau,t}^{\text{lo}}$ and $\psi_{l,\tau,t}^{\text{up}}$

I. INTRODUCTION

THE primary goal of transmission expansion planning (TEP) is to determine the optimal locations and timing for building future transmission facilities to meet specific objectives and constraints related to future load, technology, and economy. To this end, past research on TEP has primarily focused on improving the comprehensiveness and accuracy of decision-making methods, addressing the impact of the increasing penetration of renewable energy sources on power systems, and developing the corresponding solution algorithms [1]. As the construction periods for power sources shorten and the integration of renewable energy sources such as wind and photovoltaic power rapidly increases, the co-optimization of transmission and generation expansion planning (GEP) becomes increasingly critical for enhancing the safety of operation, reliability, and economic efficiency of power systems [2], [3].

Some studies on the co-optimization of TEP and GEP examine the effects of renewable energy sources and load un-

certainties [4], [5]. Centralized optimization decisions for expanding transmission lines and generators can enhance the capacity of the power system to achieve energy balance [6]. This can be accomplished by using a data-driven ambiguity set [7] within the framework of either two-stage robust optimization [8], [9] or distributionally robust optimization [7]. Furthermore, [10] and [11] focus on accelerating solutions by simplifying complex scenarios and data through clustering. Improving system reliability remains a key objective in the co-optimization of TEP and GEP [12]. In [13], evaluation indicators such as loss of load probability are integrated into the TEP model to improve the system reliability. Alternatively, multi-objective optimization models are established targeting both economy and reliability [14]. Additionally, increasing attention is paid to strengthening the power system resilience against extreme events [15]. Stochastic co-optimization is employed to improve resilience and enhance fault recovery capacity by utilizing conditional value at risk in response to issues of load shedding during extreme weather and natural disasters [16], [17]. The final transmission expansion plan must undergo comprehensive security verification including $N-1$ and $N-m-1$ contingency analyses, stability assessments, and other compliance checks by Transmission System Security Standards [18].

However, as the power system evolves, its equivalent impedance will progressively decrease, while the source of short-circuit current will continue to increase. Once the short-circuit level exceeds the nominal interrupting rating of the circuit breaker, there will be a serious safety risk for the power system. Consequently, it is essential to incorporate the short-circuit constraints (SCCs) into the co-optimization of TEP and GEP [19]. Current research proposes various methods to limit the short-circuit level such as installing superconducting fault current limiters (SFCLs) at generator buses [20], [21]. The optimal placement of SFCLs in the power system is determined by the sensitivity index of rotor angular differences [22]. In [23], SCCs are integrated into TEP to optimize grid topological expansion and curb the increase in the short-circuit level. Furthermore, since generators are the primary contributors to the short-circuit level, the expansion of new generators presents a greater challenge to the SCCs than the TEP. The calculation of short-circuit level in systems composed of synchronous generators can be conducted using the equivalent voltage source (EVS) method [24]. However, the EVS method is not directly applicable to describe the doubly-fed induction generator (DFIG) or the three-phase inverter-based distributed generator (IBDG) that are commonly integrated into wind turbine generators [25]. Therefore, the impacts of transmission lines, synchronous generators, and wind turbine generators on the SCCs should be considered in GEP [26] and the co-optimization of TEP and GEP [19].

Meanwhile, the gradual deregulation of the electricity market presents new challenges for the co-optimization of TEP and GEP. The centralized optimization in some of the above

studies does not consider the separation of decision-making entities of TEP and GEP under a deregulated environment with the establishment of the electricity market [27]. In this context, the transmission company affects the expansion decisions of the generation company by influencing locational marginal prices (LMPs) [26], while the generation company could in turn pose an impact on the expansion of lines by allocating the transmission cost [28] or cooperatively bearing part of the investment costs for lines [29]. Therefore, the generation company focuses solely on developing investment strategies aiming at maximizing its profits, without considering system-level constraints such as load balance and short-circuit level safety [30], which are critical for the transmission company. Therefore, it is crucial to separate the decision-making entities of TEP and GEP in establishing a co-optimization method that adapts to a deregulated environment.

The TEP and GEP are normally NP-hard mixed-integer linear programming (MILP) problems [31]. When considering the separation of decision-making entities, the co-optimization of TEP and GEP should be formulated as multiple separate MILP problems, with decision variables exchanged among them. Consequently, the overall problem involves TEP, GEP, and a market clearing problem, rendering a complex tri-level MILP problem, wherein the GEP is formulated as a multi-entity equilibrium problem. It is evident that this tri-level MILP problem cannot be solved directly and needs to be restructured into a bi-level problem using tools such as Karush-Kuhn-Tucker (KKT) optimality conditions. During this transformation, the complex non-convex term involving the multiplication of the continuous variables also needs to be addressed [32].

This paper proposes a multi-period co-optimization method of transmission and wind turbine GEP with SCCs under a deregulated environment, formulated as a tri-level MILP problem. The impacts of transmission lines, synchronous generators, and wind turbine generators on SCCs are integrated into the TEP model at the first level. The second and third levels are restructured into an equilibrium problem with equilibrium constraints (EPEC) using KKT optimality conditions and the single-level equivalent with bilinear terms. The EPEC is combined with the first level to create an MILP with Nash equilibrium (NE) conditions (MILP-NE) through complementarity problem reformulation (CPR). An iterative algorithm targeting SCCs is also proposed, which updates the EPEC decision set via the diagonalization method (DM). Case studies demonstrate that the proposed method effectively addresses the separation of decision-making entities for TEP and GEP under a deregulated environment, ensuring that the multi-period planning results meet the SCCs.

The remainder of this paper is organized as follows. Section II provides the outline of the proposed method. Section III presents the mathematical formulation. Section IV describes the solution algorithm. Section V presents simulation studies. Finally, Section VI concludes this paper.

II. OUTLINE OF PROPOSED METHOD

The overall framework of the proposed method is illustrated in Fig. 1. The problem is described as a tri-level MILP problem, with the decision-making entities being the transmission company, generation companies, and the independent system operator, respectively.

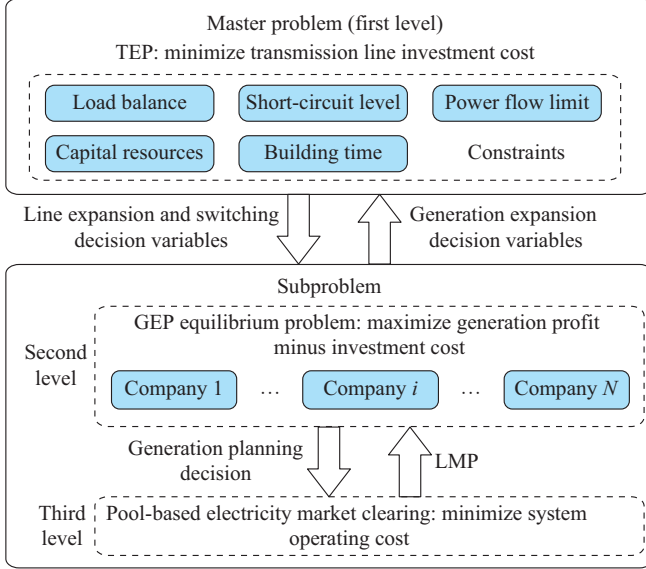


Fig. 1. Overall framework of proposed method.

A. Master Problem

The first level serves as the master problem, defined as a TEP model governed by binary variables. The objective of the master problem is to minimize the transmission line investment cost while meeting all operating demands of the power system. This problem is subject to constraints such as the load balance, the SCCs, the limit of power flow, etc. The generator expansion decision variables from the subproblem are treated as fixed parameters in the master problem, while the line expansion and switching decision variables solved in the master problem are passed to the subproblem.

B. Subproblem

The subproblem includes GEP and electricity market clearing, represented as the second and third levels, respectively. The second level deals with a GEP equilibrium problem governed by binary variables, aiming to maximize the investment profit of each generation entity. Given the non-universal implementation of the capacity market and the largely uncorrelated nature of its benefits with the TEP, this paper excludes the consideration of capacity market benefits. The decision variables for lines and generators from the first and second levels are treated as fixed parameters at the third level. The third level focuses on the electricity market clearing problem to minimize system operating cost and determine the LMPs at each bus. The LMPs obtained from the third level are then passed to the second level as parameters, and the GEP decisions from the second level are fed back to the master problem.

III. MATHEMATICAL FORMULATION

A. Short-circuit Analysis

Among various types of short-circuit faults, the three-phase short-circuit fault undoubtedly represents the most severe condition in terms of the magnitude of short-circuit level. Therefore, this paper primarily investigates the issue of the most critical three-phase short-circuit level with all generators online. The Δ -circuit of the synchronous generator is passive everywhere except at the fault location. This means only the sub-transient, transient, or steady-state impedances X_g'' are kept in the Δ -circuit, while their ideal voltage sources are annulled, as shown in Fig. 2(a). Hence, the short-circuit level can be approximated as $I_F^f = 1/Z_{FF}$.

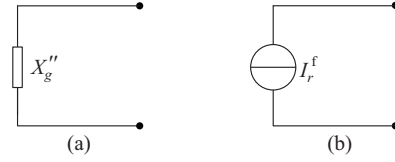


Fig. 2. Δ -circuit of different generators. (a) Synchronous generator. (b) DFIG and IBDG.

However, the Δ -circuits for DFIG and IBDG are more complex. Disregarding the crowbar protection of DFIG, both DFIG and IBDG can be modeled as ideal current sources that continuously supply a fixed current I_r^f during short-circuit faults, as shown in Fig. 2(b). The magnitude of the short-circuit level is contingent upon the control strategy of the power electronic devices. Strategy I maintains the same pre-fault currents throughout the fault. Strategy II provides additional reactive current to support the voltage. It is evident that Strategy II has a more significant impact on the short-circuit level, with the maximum fault current being 1-1.5 of the rated current in most cases [33]. In Strategy II, parts of the currents supplied by DFIG and IBDG that exceed their pre-fault currents (excess currents) need to be injected into the Δ -circuit [34]. The fault circuit can be decomposed into the following two equivalent systems: $U_F^0 = \sum_{i \in \mathcal{N}} I_i^0 Z_{iF}$, $\Delta U_F = \Delta I_F^f Z_{FF} + \sum_{r \in \mathcal{C}^N} I_r^f Z_{\text{bus}(r), F}$. For a three-phase short-circuit fault, $U_F^0 + \Delta U_F = 0$. Hence, the short-circuit level I_F^f can be expressed as $I_F^f = \Delta I_F^f = -\frac{1}{Z_{FF}} \left(\sum_{r \in \mathcal{C}^N} I_r^f Z_{\text{bus}(r), F} + \sum_i I_i^0 Z_{iF} \right)$.

U_F^0 depends on the actual operating conditions of the power system. During planning studies, only grid topology constraints are considered in the calculations of short-circuit level, excluding the operational control under specific conditions. We therefore assume a nominal pre-fault voltage of 1 p.u. [23] (adjustable if needed) and account solely for the reactance components X_{ij} in the system admittance matrix. Consequently, an approximate formula for calculating the value of short-circuit level can be derived as:

$$I_F^f = \frac{\sum_{r \in \mathcal{C}^N} I_r^f X_{\text{bus}(r), F} + 1}{X_{FF}} \quad (1)$$

Considering the worst-case scenario, the currents injected

by DFIG and IBDG into the Δ -circuit are $I_r^f = 1.5I_r^N$.

B. Admittance Matrix Analysis

Upon the addition of a line with reactance ΔX_l between buses i and j , the m^{th} -row and n^{th} -column element X_{mn} of the admittance matrix is expressed as:

$$X_{mn} = X_{mn}^0 - \frac{(X_{mi}^0 - X_{mj}^0)(X_{ni}^0 - X_{nj}^0)}{X_{ii}^0 + X_{jj}^0 - 2X_{ij}^0 + \Delta X_l} \quad (2)$$

When an additional synchronous generator with a sub-synchronous reactance of ΔX_g is introduced at bus i , the element X_{mn} will correspondingly change as:

$$X_{mn} = X_{mn}^0 - \frac{X_{mi}^0 X_{ni}^0}{X_{ii}^0 + \Delta X_g} \quad (3)$$

The short-circuit level, considering the expansion of transmission lines and generators, is thereby derived.

$$\sum_{r \in \mathcal{C}^w} 1.5I_r^N (X_{\text{bus}(r),F}^0 + \Delta X_{\text{bus}(r),F}) + 1 \leq (X_{FF}^0 + \Delta X_{FF}) I_F^{\text{Sc}} \quad (4)$$

$$\Delta X_{FF} = - \sum_g \frac{u_g (X_{F,\text{bus}(g)}^0)^2}{X_{\text{bus}(g),\text{bus}(g)}^0 + \Delta X_g} - \sum_{l \in \mathcal{L}_{\text{candi}}} \frac{v_l (X_{F,\text{fr}(l)}^0 - X_{F,\text{to}(l)}^0)^2}{X_{\text{fr}(l),\text{fr}(l)}^0 + X_{\text{to}(l),\text{to}(l)}^0 - 2X_{\text{fr}(l),\text{to}(l)}^0 + \Delta X_l} - \sum_{l \in \mathcal{L}_{\text{exist}}} \frac{(w_l - 1)(X_{F,\text{fr}(l)}^0 - X_{F,\text{to}(l)}^0)^2}{X_{\text{fr}(l),\text{fr}(l)}^0 + X_{\text{to}(l),\text{to}(l)}^0 - 2X_{\text{fr}(l),\text{to}(l)}^0 + \Delta X_l} \quad (5)$$

$$\Delta X_{\text{bus}(r),F} = - \sum_g \frac{u_g X_{\text{bus}(r),\text{bus}(g)}^0 X_{F,\text{bus}(g)}^0}{X_{\text{bus}(g),\text{bus}(g)}^0 + \Delta X_g} - \sum_{l \in \mathcal{L}_{\text{candi}}} \frac{v_l (X_{\text{bus}(r),\text{fr}(l)}^0 - X_{\text{bus}(r),\text{to}(l)}^0)(X_{F,\text{fr}(l)}^0 - X_{F,\text{to}(l)}^0)}{X_{\text{fr}(l),\text{fr}(l)}^0 + X_{\text{to}(l),\text{to}(l)}^0 - 2X_{\text{fr}(l),\text{to}(l)}^0 + \Delta X_l} - \sum_{l \in \mathcal{L}_{\text{exist}}} \frac{(w_l - 1)(X_{\text{bus}(r),\text{fr}(l)}^0 - X_{\text{bus}(r),\text{to}(l)}^0)(X_{F,\text{fr}(l)}^0 - X_{F,\text{to}(l)}^0)}{X_{\text{fr}(l),\text{fr}(l)}^0 + X_{\text{to}(l),\text{to}(l)}^0 - 2X_{\text{fr}(l),\text{to}(l)}^0 + \Delta X_l} \quad (6)$$

I_r^N can be represented by the rated installed capacity \bar{P}_r^G .

C. First Level

Initially, the TEP model is given as:

$$\min \sum_{t \in \mathcal{T}} \sum_{l \in \mathcal{L}_{\text{candi}}} IC_l^L \cdot (v_{l,t} - v_{l,t-1}) \quad (7)$$

s.t.

$$v_{l,t-1} \leq v_{l,t} \quad \forall l \in \mathcal{L}_{\text{candi}}, \forall t \in \mathcal{T}, t \geq 2 \quad (8)$$

$$\sum_{l \in \mathcal{L}_{\text{candi}}} IC_l^L \cdot (v_{l,t} - v_{l,t-1}) \leq LCM_t \quad \forall t \in \mathcal{T} \quad (9)$$

$$\sum_{l \in \mathcal{L}_{\text{candi}}} \bar{P}_l^f (v_{l,t} - v_{l,t-1}) \leq LFM_t \quad \forall t \in \mathcal{T} \quad (10)$$

$$\sum_{l \in \mathcal{L}_{\text{candi}}} (v_{l,t} - v_{l,t-1}) \leq LNM_t \quad \forall t \in \mathcal{T} \quad (11)$$

$$v_{l,t} = 0 \quad \forall l \in \mathcal{L}_{\text{candi}}, \forall t \in \mathcal{T}, t \leq T_l^{\text{max}} \quad (12)$$

$$w_{l,t} - w_{l,t-1} = y_{l,t} \quad \forall l \in \mathcal{L}_{\text{exist}}, \forall t \in \mathcal{T} \quad (13)$$

$$w_{l,t-1} - w_{l,t} = z_{l,t} \quad \forall l \in \mathcal{L}_{\text{exist}}, \forall t \in \mathcal{T} \quad (14)$$

$$\sum_{l \in \mathcal{L}_{\text{exist}}} (y_{l,t} + z_{l,t}) \leq SNM_t \quad \forall t \in \mathcal{T} \quad (15)$$

$$\sum_{\tau = \max(0, t - M_l + 1)}^t y_{l,\tau} \leq w_{l,t} \quad \forall l \in \mathcal{L}_{\text{exist}}, \forall t \in \mathcal{T} \quad (16)$$

$$\sum_{\tau = \max(0, t - MD_l + 1)}^t z_{l,\tau} \leq 1 - w_{l,t} \quad \forall l \in \mathcal{L}_{\text{exist}}, \forall t \in \mathcal{T} \quad (17)$$

$$(4)-(6) \quad (18)$$

Formulas (8)-(12) place constraints on the binary variables for candidate lines; (9)-(11) specify the maximum annual cost, capacity, and quantity for newly expanded lines, respectively; (12) represents the construction period; (13)-(15) impose similar constraints for the binary variables of line switching; (16) and (17) define the minimum durations of offline and online states, respectively; and (18) sets the SCCs. We adopt a deregulated environment where the operation and investment of transmission network are managed by an independent operator. Consequently, the proposed objective function excludes the system operating costs.

D. Second Level

A wind farm consists of multiple components including wind turbines, collector lines, control center, step-up equipment, and grid-connected lines. Notably, the costs of step-up equipment and grid-connected lines are significant [35]. However, the TEP typically does not account for individual wind farm topologies. To simplify modeling and computation, the TEP model consolidates all internal wind farm construction costs (including grid-connected expenses) into a single cost component, given the relatively uniform grid connection topology of individual wind farms. The grid-connected points for candidate wind farms are assumed based on geographical factors, eliminating the need for separate grid integration studies.

To maximize the generation profit, the GEP model for a synchronous generator is formulated as:

$$\max Gpr_g^G \quad (19)$$

s.t.

$$Gpr_g^G = \sum_{\forall t \in \mathcal{T}} \sum_{\tau \in \Omega_t} \Gamma_{\tau} (\lambda_{\text{bus}(g),\tau,t} - PC_g^G) P_{g,\tau,t}^g - C_n^{\text{Eq}} \cdot IC_g^G \cdot \sum_{\forall t \in \mathcal{T}} u_{g,t} \quad \forall g \in \mathcal{C}_{\text{candi}}^G \quad (20)$$

$$u_{g,t-1} \leq u_{g,t} \quad \forall g \in \mathcal{C}_{\text{candi}}^G, \forall t \in \mathcal{T}, t \geq 2 \quad (21)$$

$$u_{g,t} = 0 \quad \forall g \in \mathcal{C}_{\text{candi}}^G, \forall t \in \mathcal{T}, t \leq T_g^{\text{max}} \quad (22)$$

Equation (20) represents the profit Gpr_g^G from the expansion of synchronous generators, and (21) and (22) impose constraints on the candidate binary variables of the generators. The model of the wind turbine generator is consistent with that of the traditional generator. This GEP is represented as a mathematical program with equilibrium constraint (MPEC) model, where the equilibrium constraints are obtained at the third level.

E. Third Level

A pool-based electricity market clearing model is established as:

$$\min \left\{ \sum_{g \in \mathcal{C}\tau \in \Omega_\tau} PC_g^G \cdot p_{g,\tau,t}^g + PC^\theta \cdot \sum_{i \in \mathcal{N}} \sum_{\tau \in \Omega_\tau} \theta_{i,\tau,t} \right\} \quad \forall t \in \mathcal{T} \quad (23)$$

s.t.

$$\mu_\tau D_{i,t} - \theta_{i,\tau,t} = \sum_{g \in \mathcal{C}} P_{g,\tau,t}^g + \sum_{l \in \mathcal{L}|\text{to}(l)=i} P_{l,\tau,t}^f - \sum_{l \in \mathcal{L}|\text{fr}(l)=i} P_{l,\tau,t}^f; (\lambda_{i,\tau,t}) \quad \forall i \in \mathcal{N}, \forall \tau \in \Omega_\tau, \forall t \in \mathcal{T} \quad (24)$$

$$-M(1-w_{l,t}) \leq p_{l,\tau,t}^f - \frac{\theta_{\text{fr}(l),\tau,t} - \theta_{\text{to}(l),\tau,t}}{x_l} \leq M(1-w_{l,t}); (v_{l,\tau,t}^{\text{lo}}, v_{l,\tau,t}^{\text{up}}) \quad \forall l \in \mathcal{L}_{\text{exist}}, \forall \tau \in \Omega_\tau, \forall t \in \mathcal{T} \quad (25)$$

$$-M(1-v_{l,t}) \leq p_{l,\tau,t}^f - \frac{\theta_{\text{fr}(l),\tau,t} - \theta_{\text{to}(l),\tau,t}}{x_l} \leq M(1-v_{l,t}); (\pi_{l,\tau,t}^{\text{lo}}, \pi_{l,\tau,t}^{\text{up}}) \quad \forall l \in \mathcal{L}_{\text{candi}}, \forall \tau \in \Omega_\tau, \forall t \in \mathcal{T} \quad (26)$$

$$-w_{l,t} \bar{P}_l^f \leq p_{l,\tau,t}^f \leq w_{l,t} \bar{P}_l^f; (\phi_{l,\tau,t}^{\text{lo}}, \phi_{l,\tau,t}^{\text{up}}) \quad \forall l \in \mathcal{L}_{\text{exist}}, \forall \tau \in \Omega_\tau, \forall t \in \mathcal{T} \quad (27)$$

$$-v_{l,t} \bar{P}_l^f \leq p_{l,\tau,t}^f \leq v_{l,t} \bar{P}_l^f; (\psi_{l,\tau,t}^{\text{lo}}, \psi_{l,\tau,t}^{\text{up}}) \quad \forall l \in \mathcal{L}_{\text{candi}}, \forall \tau \in \Omega_\tau, \forall t \in \mathcal{T} \quad (28)$$

$$0 \leq p_{g,\tau,t}^g \leq \bar{P}_g^G; (\gamma_{g,\tau,t}^{\text{lo}}, \gamma_{g,\tau,t}^{\text{up}}) \quad \forall g \in \mathcal{C}_{\text{exist}}^G, \forall \tau \in \Omega_\tau, \forall t \in \mathcal{T} \quad (29)$$

$$0 \leq p_{g,\tau,t}^g \leq u_{g,t} \bar{P}_g^G; (\zeta_{g,\tau,t}^{\text{lo}}, \zeta_{g,\tau,t}^{\text{up}}) \quad \forall g \in \mathcal{C}_{\text{candi}}^G, \forall \tau \in \Omega_\tau, \forall t \in \mathcal{T} \quad (30)$$

$$0 \leq p_{g,\tau,t}^g \leq u_{g,t} \alpha_\tau \bar{P}_g^G; (\zeta_{g,\tau,t}^{\text{lo}}, \zeta_{g,\tau,t}^{\text{up}}) \quad \forall g \in \mathcal{C}_{\text{candi}}^W, \forall \tau \in \Omega_\tau, \forall t \in \mathcal{T} \quad (31)$$

$$\theta_{i,\tau,t} \geq 0; (\omega_{i,\tau,t}) \quad \forall i \in \mathcal{N}, \forall \tau \in \Omega_\tau, \forall t \in \mathcal{T} \quad (32)$$

The objective function (23) minimizes the system operating cost; (24) represents the power balance equation of buses; (25)-(28) constrain the transmission power of lines controlled by decision variables at the first level; and (29)-(31) are the output limitations for the generators, where candidate generators are controlled by decision variables at the second level. The terms within parentheses are the dual variables corresponding to the constraints.

IV. SOLUTION ALGORITHM

The tri-level MILP problem consists of MILP models at the first two levels and a linear programming model at the third level. The above problem is rewritten as an MILP-NE, and an iterative algorithm targeting SCCs is proposed to solve it. Four main steps are included: ① merging the subproblem using the KKT optimality conditions; ② handling bilinear terms in the objective function of the subproblem and establishing the MPEC model for each generator; ③ formulating the NE conditions for the subproblem by CPR; and ④ proposing an iterative algorithm targeting SCCs.

A. Step 1

The KKT optimality conditions for the market clearing model at the third level are given as:

$$(24)-(32) \quad (33)$$

$$v_{l,\tau,t}^{\text{lo}}, v_{l,\tau,t}^{\text{up}}, \pi_{l,\tau,t}^{\text{lo}}, \pi_{l,\tau,t}^{\text{up}}, \phi_{l,\tau,t}^{\text{lo}}, \phi_{l,\tau,t}^{\text{up}}, \psi_{l,\tau,t}^{\text{lo}}, \psi_{l,\tau,t}^{\text{up}}, \gamma_{g,\tau,t}^{\text{lo}}, \gamma_{g,\tau,t}^{\text{up}}, \zeta_{g,\tau,t}^{\text{lo}}, \zeta_{g,\tau,t}^{\text{up}}, \omega_{i,\tau,t} \geq 0 \quad (34)$$

$$PC_g^G - \lambda_{\text{bus}(g),\tau,t} - \gamma_{g,\tau,t}^{\text{lo}} + \gamma_{g,\tau,t}^{\text{up}} = 0 \quad \forall g \in \mathcal{C}_{\text{exist}}^G, \forall \tau \in \Omega_\tau, \forall t \in \mathcal{T} \quad (35)$$

$$PC_g^G - \lambda_{\text{bus}(g),\tau,t} - \zeta_{g,\tau,t}^{\text{lo}} + \zeta_{g,\tau,t}^{\text{up}} = 0 \quad \forall g \in \mathcal{C}_{\text{candi}}^G, \forall \tau \in \Omega_\tau, \forall t \in \mathcal{T} \quad (36)$$

$$PC_g^G - \lambda_{\text{bus}(g),\tau,t} - \zeta_{g,\tau,t}^{\text{lo}} + \zeta_{g,\tau,t}^{\text{up}} = 0 \quad \forall g \in \mathcal{C}_{\text{candi}}^W, \forall \tau \in \Omega_\tau, \forall t \in \mathcal{T} \quad (37)$$

$$\lambda_{\text{to}(l),\tau,t} - \lambda_{\text{fr}(l),\tau,t} - v_{l,\tau,t}^{\text{lo}} + v_{l,\tau,t}^{\text{up}} - \phi_{l,\tau,t}^{\text{lo}} + \phi_{l,\tau,t}^{\text{up}} = 0 \quad \forall l \in \mathcal{L}_{\text{exist}}, \forall \tau \in \Omega_\tau, \forall t \in \mathcal{T} \quad (38)$$

$$\lambda_{\text{to}(l),\tau,t} - \lambda_{\text{fr}(l),\tau,t} - \pi_{l,\tau,t}^{\text{lo}} + \pi_{l,\tau,t}^{\text{up}} - \psi_{l,\tau,t}^{\text{lo}} + \psi_{l,\tau,t}^{\text{up}} = 0 \quad \forall l \in \mathcal{L}_{\text{candi}}, \forall \tau \in \Omega_\tau, \forall t \in \mathcal{T} \quad (39)$$

$$- \sum_{l \in \mathcal{L}_{\text{exist}}|\text{fr}(l)=i} \frac{-v_{l,\tau,t}^{\text{lo}} + v_{l,\tau,t}^{\text{up}}}{x_l} + \sum_{l \in \mathcal{L}_{\text{exist}}|\text{to}(l)=i} \frac{-v_{l,\tau,t}^{\text{lo}} + v_{l,\tau,t}^{\text{up}}}{x_l} - \sum_{l \in \mathcal{L}_{\text{candi}}|\text{fr}(l)=i} \frac{-\pi_{l,\tau,t}^{\text{lo}} + \pi_{l,\tau,t}^{\text{up}}}{x_l} + \sum_{l \in \mathcal{L}_{\text{candi}}|\text{to}(l)=i} \frac{-\pi_{l,\tau,t}^{\text{lo}} + \pi_{l,\tau,t}^{\text{up}}}{x_l} = 0 \quad \forall i \in \mathcal{N}, \forall \tau \in \Omega_\tau, \forall t \in \mathcal{T} \quad (40)$$

$$\begin{aligned} & \sum_{g \in \mathcal{C}\tau \in \Omega_\tau} PC_g^G \cdot p_{g,\tau,t}^g + PC^\theta \cdot \sum_{i \in \mathcal{N}} \sum_{\tau \in \Omega_\tau} \theta_{i,\tau,t} = \\ & \sum_{i \in \mathcal{N}} \sum_{\tau \in \Omega_\tau} \mu_\tau D_{i,t} \lambda_{i,\tau,t} - \sum_{l \in \mathcal{L}_{\text{exist}} \tau \in \Omega_\tau} M(1-w_{l,t})(v_{l,\tau,t}^{\text{up}} + v_{l,\tau,t}^{\text{lo}}) - \\ & \sum_{l \in \mathcal{L}_{\text{candi}} \tau \in \Omega_\tau} M(1-v_{l,t})(\pi_{l,\tau,t}^{\text{up}} + \pi_{l,\tau,t}^{\text{lo}}) - \\ & \sum_{l \in \mathcal{L}_{\text{exist}} \tau \in \Omega_\tau} w_{l,t} \bar{P}_l^f (\phi_{l,\tau,t}^{\text{up}} + \phi_{l,\tau,t}^{\text{lo}}) - \sum_{\tau \in \Omega_\tau} v_{l,t} \bar{P}_l^f (\psi_{l,\tau,t}^{\text{up}} + \psi_{l,\tau,t}^{\text{lo}}) - \\ & \sum_{g \in \mathcal{C}_{\text{exist}}^G \tau \in \Omega_\tau} \bar{P}_g^G \gamma_{g,\tau,t}^{\text{up}} - \sum_{g \in \mathcal{C}_{\text{candi}}^G \tau \in \Omega_\tau} u_{g,t} \bar{P}_g^G \zeta_{g,\tau,t}^{\text{up}} - \\ & \sum_{g \in \mathcal{C}_{\text{candi}}^W \tau \in \Omega_\tau} u_{g,t} \alpha_\tau \bar{P}_g^G \zeta_{g,\tau,t}^{\text{up}} \quad \forall t \in \mathcal{T} \end{aligned} \quad (41)$$

Equation (34) enforces the non-negativity constraint on the dual variables associated with inequality constraints; (35)-(40) delineate the first-order conditions of the Lagrangian function of the primal problem; and (41) establishes the condition of strong duality by equating the objective function value of the primal problem to that of the dual problem.

The non-convex term is linearized by introducing the continuous auxiliary variable $a_{l,\tau,t}^{\text{up}}$ as:

$$\begin{cases} -Mw_{l,t} \leq a_{l,\tau,t}^{\text{up}} \leq Mw_{l,t} \\ -M(1-w_{l,t}) \leq v_{l,\tau,t}^{\text{up}} - a_{l,\tau,t}^{\text{up}} \leq M(1-w_{l,t}) \end{cases} \quad (42)$$

The remaining product terms are linearized in the same manner as described in (42).

The optimization problem at the third level is restructured into constraints at the second level using the KKT optimality conditions, thus restructuring the tri-level MILP problem into a bi-level problem.

B. Step 2

Equation (20) shows that merging the third level with the second level results in non-convex terms $\lambda_{\text{bus}(g),\tau,t} p_{g,\tau,t}^g$ from the multiplication of two continuous variables [32].

From (36), we have $(\lambda_{\text{bus}(g),\tau,t} - PC_g^G) p_{g,\tau,t}^g = (\zeta_{g,\tau,t}^{\text{up}} - \zeta_{g,\tau,t}^{\text{lo}}) \cdot p_{g,\tau,t}^g, \forall g \in \mathcal{C}_{\text{candi}}^G$. Considering the complementary slackness conditions of the third level, we have $(p_{g,\tau,t}^g - u_{g,t} \bar{P}_g^G) \perp \zeta_{g,\tau,t}^{\text{up}}$,

and $(0 - p_{g,\tau,t}^g) \perp \zeta_{g,\tau,t}^{\text{lo}}$. Then, we can derive $(\zeta_{g,\tau,t}^{\text{up}} - \zeta_{g,\tau,t}^{\text{lo}}) p_{g,\tau,t}^g = u_{g,t} \bar{P}_g^G \zeta_{g,\tau,t}^{\text{up}}$. Consequently, (20) is restructured as:

$$Gpr_g^G = \sum_{\forall t \in \mathcal{T}} \sum_{\tau \in \Omega_\tau} \Gamma_\tau u_{g,t} \bar{P}_g^G \zeta_{g,\tau,t}^{\text{up}} - C_n^{\text{Eq}} \cdot IC_g^G \cdot \sum_{\forall t \in \mathcal{T}} u_{g,t} \quad \forall g \in \mathcal{C}_{\text{candi}}^G \quad (43)$$

For the wind turbine generators, Gpr_g^G can be linearized in the same manner as:

$$Gpr_g^G = \sum_{\forall t \in \mathcal{T}} \sum_{\tau \in \Omega_\tau} \Gamma_\tau u_{g,t} \alpha_{\tau,t} \bar{P}_g^G \zeta_{g,\tau,t}^{\text{up}} - C_n^{\text{Eq}} \cdot IC_g^G \cdot \sum_{\forall t \in \mathcal{T}} u_{g,t} \quad \forall g \in \mathcal{C}_{\text{candi}}^W \quad (44)$$

The MPEC models for each synchronous generator and wind turbine generator are established, comprising the investment objective function (19), the constraint conditions (20)-(22), and the market clearing equilibrium conditions (33)-(41).

C. Step 3

The MPEC problems of generators collectively form an EPEC problem. The equilibrium solution can be obtained through the DM if it exists. Alternatively, the CPR can be employed to derive a mixed complementarity problem. The optimal solution obtained by this approach is a necessary but not sufficient condition for the NE of the original EPEC problem, i. e., a stationary point. Since the EPEC problem may not have a pure NE solution, or it may exist but lead to an infeasible master problem, we relax the master problem to some extent. The objective is to find a promising multi-period transmission expansion plan.

$$\min \sum_{t \in \mathcal{T}} \sum_{l \in \mathcal{L}_{\text{candi}}} IC_l^L \cdot (v_{l,t} - v_{l,t-1}) + M^\varepsilon \sum_{t \in \mathcal{T}} \sum_{i \in \mathcal{N}} \bar{\varepsilon}_{i,t} \quad (45)$$

$$\sum_{r \in \mathcal{C}^N} 1.5I_r^N (X_{\text{bus}(r),F}^0 + \Delta X_{\text{bus}(r),F}) + 1 \leq (X_{FF}^0 + \Delta X_{FF})(I_F^{\text{Sc}} + \bar{\varepsilon}_{i,t}) \quad (46)$$

$$\bar{\varepsilon}_{i,t} \geq 0 \quad \forall i \in \mathcal{N}, \forall t \in \mathcal{T} \quad (47)$$

The SCCs are relaxed and integrated into the objective function as penalty terms.

For each MPEC problem, its NE conditions are given as:

$$Gpr_g^G(u_{g,t}) \geq Gpr_g^G(u_{g,t}^{s_g}, u_{-g,t}) \quad \forall g \in \mathcal{C}_{\text{candi}}^G \cup \mathcal{C}_{\text{candi}}^W, \forall s_g \in \mathcal{S}_g \quad (48)$$

The left-hand side (LHS) utility function is shown in (43) and (44) for the synchronous generator and wind turbine generator, respectively. The right-hand side (RHS) utility function is calculated based on the fixed investment decision of the generator as:

$$Gpr_g^G(u_{g,t}^{s_g}, u_{-g,t}) = \sum_{\forall t \in \mathcal{T}} \sum_{\tau \in \Omega_\tau} \Gamma_\tau u_{g,t}^{s_g} \bar{P}_g^G \zeta_{g,\tau,t}^{\text{up}} - C_n^{\text{Eq}} \cdot IC_g^G \cdot \sum_{\forall t \in \mathcal{T}} u_{g,t}^{s_g} \quad \forall g \in \mathcal{C}_{\text{candi}}^G, \forall s_g \in \mathcal{S}_g \quad (49)$$

The utility function for the wind turbine generator is analogous.

We assume that the decisions of all generators are optimal for the EPEC problem on the LHS. On the RHS, a set of constraints is evaluated for all decisions within \mathcal{S}_g and for each generator, where the decisions of the competitors ($-g$) are fixed in the optimal solution for the MPEC problem. The detailed constraints are provided in Supplementary Material A.

D. Step 4

The subproblem and the master problem are restructured into an MILP-NE by the CPR. Since the CPR requires iterating all decisions for the generator, there are $T+1$ feasible decisions for each generator when the planning period is T at most. To reduce the complexity, we propose an iterative algorithm targeting SCCs that combines DM and CPR. Considering that the decisions of the subproblem primarily alter the SCCs of the master problem, we establish a clear termination condition for the proposed iterative algorithm targeting SCCs, i.e., satisfying the short-circuit-level constraint (4).

1) Set $k=0$. Initialize the decision set of each generator $\mathcal{H}^k = \{u_{g,t}^{s_g} = 0 | \forall t \in \mathcal{T}, \forall g \in \mathcal{C}_{\text{candi}}^G \cup \mathcal{C}_{\text{candi}}^W, \forall s_g \in \mathcal{S}_g\}$, $\mathcal{S}_g^k = \{k\}$.

2) Solve the MILP-NE problem with the decision set \mathcal{S}_g^k . Report TEP solution $\mathcal{V}^k = \{v_{l,t}^k | \forall l \in \mathcal{L}_{\text{candi}}, \forall t \in \mathcal{T}\}$ and $\mathcal{W}^k = \{w_{l,t}^k | \forall l \in \mathcal{L}_{\text{exist}}, \forall t \in \mathcal{T}\}$. Solve the EPEC subproblem with DM by fixing the $\mathcal{V}^k + \mathcal{W}^k$ and report the NE solution $\mathcal{U}^k = \{u_{g,t}^k | \forall g \in \mathcal{C}_{\text{candi}}^G \cup \mathcal{C}_{\text{candi}}^W, \forall t \in \mathcal{T}\}$.

3) Check the constraint (4). If SCCs are satisfied, output the solution $\mathcal{V}^k + \mathcal{W}^k$ and exit the iteration. Otherwise, go to the previous step.

4) If $\mathcal{U}^k \notin \mathcal{H}^k$, go to the next step. Otherwise, the feasible solution satisfying SCCs is unavailable. Output the relaxation optimal solution $\mathcal{V}^k + \mathcal{W}^k$ and exit the iteration.

5) Let $k=k+1$, add \mathcal{U}^k to \mathcal{H}^k , and $\mathcal{S}_g^k = \{k\} + \mathcal{S}_g^{k-1}$. Add a constraint (50) to the MILP-NE for cutting $\mathcal{V}^k + \mathcal{W}^k$, and go to 2).

$$\sum_{l \in \mathcal{L}_{\text{candi}}, t \in \mathcal{T}} |v_{l,t} - v_{l,t}^k| + \sum_{l \in \mathcal{L}_{\text{exist}}, t \in \mathcal{T}} |w_{l,t} - w_{l,t}^k| \geq 1 \quad (50)$$

The proposed iterative algorithm targeting SCCs is not guaranteed to find a global optimal solution of the tri-level MILP problem. But it can find a promising multi-period transmission expansion plan.

The growing load demand and new generation expansion may create conflicts between power balance requirements and SCCs. When such conflicts occur, the proposed iterative algorithm targeting SCCs offers a practical solution by providing an optimized compromise that minimizes the short-circuit level. This ensures feasible planning outcomes while maintaining system security, significantly improving the grid planning flexibility. The specific computational steps of DM are presented in Supplementary Material B.

V. SIMULATION

This section examines the proposed method on the modified IEEE 24-bus reliability test system (RTS) [36], as shown in Fig. 3. The load duration curve consists of two parts, with 100% and 65% load levels lasting for half of the time, respectively. The construction time is two years, with the planning target being the transmission lines and generators for two years later. The annual investment limit for lines is 150 M\$, with no limit on the number of lines. Constrained by load forecasting capabilities, the guiding value of overly long-term planning is diminished. This paper adopts a four-year short-term planning horizon. The candidate lines

consist of all existing lines and five new connection routes. The nominal interrupting ratings of the circuit breaker are assumed to be 30 kA and 35 kA for 138 kV and 230 kV voltage levels, respectively. The discount rate is supposed to be 5%. The annual load growth rate is assumed to be 9%.

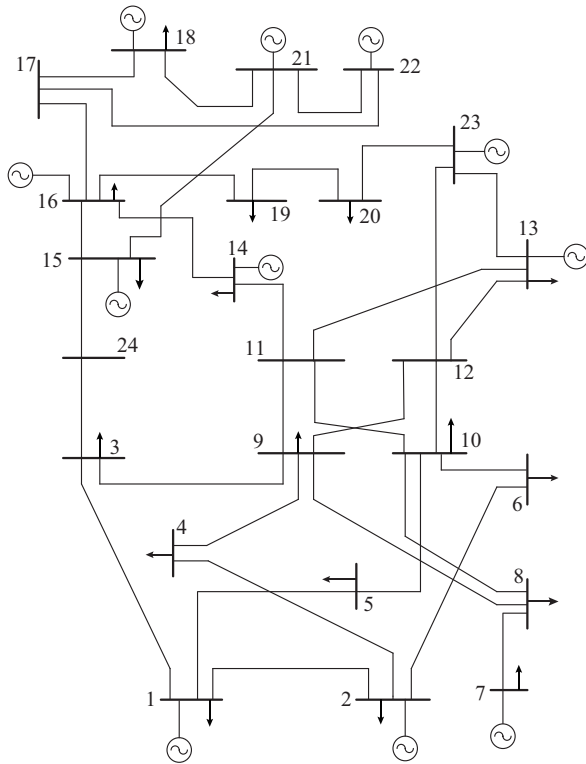


Fig. 3. Modified IEEE 24-bus RTS.

The problem is solved by using the 12th Gen Intel® Core® i7-12700 2.10 GHz with 16 GB of RAM, and the algorithm is implemented by using the Python language version 3.10.9.

The following cases are conducted in the simulation.

1) Case 1: multi-period co-optimization of transmission and wind turbine GEP with SCCs under a deregulated environment, namely the proposed method.

2) Case 2: multi-period TEP excluding SCCs and the influence of GEP under a deregulated environment.

3) Case 3: multi-period TEP with SCCs excluding the influence of GEP under a deregulated environment. For the sake of comparison, the GEP results are acquired later based on the result of the TEP.

4) Case 4: multi-period TEP and GEP adopting a centralized method with SCCs. In this case, the expansion of transmission lines and generators is centrally optimized to minimize the expansion investment cost and system operating cost in total. For the sake of comparison, the separate decision-making results of GEP based on maximizing the profit of entity will be obtained later using the results from TEP.

The comparison of the settings for Cases 1-4 is shown in Table I. The comparison between Cases 1 and 2 is used to verify the effectiveness of SCCs in planning for short-circuit-level control. The comparison among Cases 1-3 is used to validate the importance of considering GEP for short-circuit-

level control. The comparison among Cases 1-4 is used to assess the impact of the separate decision-making entities of TEP and GEP under a deregulated environment on short-circuit-level control.

TABLE I
COMPARISON OF SETTINGS FOR CASES 1-4

Case	Condition setting		
	SCC	GEP	Deregulated environment
Case 1	√	√	√
Case 2	×	×	×
Case 3	√	×	√
Case 4	√	√	×

A. Results of Case 1

Table II illustrates the results of line expansion and switching for the next four years. In the first year, the grid topology is optimized by adding four new lines. In the second and third years, two new lines are invested annually. And five new lines are added in year 4. Table III demonstrates that new line expansions in year 1 prompt investments in both synchronous generators (buses 8, 13, 17, and 18) and wind turbine generators (buses 16, 21, 22, and 23). Additionally, the line expansions in the fourth year result in the installation of a synchronous generator at bus 22.

TABLE II
RESULTS OF LINE EXPANSION AND SWITCHING FOR NEXT FOUR YEARS

Period	Invested line	Switched-on line	Switched-off line
Year 1	11-20, 12-22, 18-19, 20-23		2-4, 8-10, 15-16, 16-19, 18-21
Year 2	10-12, 11-13	2-4, 8-10, 15-16, 16-19	1-3, 1-5, 16-19, 21-22
Year 3	10-11, 20-22	1-3, 18-21, 21-22	1-2, 15-16, 17-18
Year 4	3-9, 9-11, 12-13, 14-16, 15-21	1-5	21-22

TABLE III
BUSES OF INVESTED GENERATORS IN CASE 1

Type	Bus (period)
Synchronous generator	8, 13, 17, 18 (year 1), 22 (year 4)
Wind turbine generator	16, 21, 22, 23 (year 1)

To prevent short-circuit-level violations, topology adjustments through line switching are required. Table II indicates that five lines remain offline annually through switching operations. These offline lines can be scheduled for maintenance and other operational purposes.

Table IV presents the short-circuit level of buses after TEP and GEP with $\Delta I^{\text{Sc}(l)} \leq 5$ kA in Case 1, where $\Delta I^{\text{Sc}} = \text{BNIR} - I^{\text{Sc}}$, BNIR is the circuit breaker nominal interrupting rating, and superscript “(1)” represents Case 1. By integrating SCCs and accounting for the GEP impacts within the TEP framework under a deregulated environment, the system ensures compliance with SCCs following transmission and generation expansion, thereby preserving the security.

TABLE IV
SHORT-CIRCUIT LEVEL OF BUSES AFTER TEP AND GEP

Bus No.	Nominal voltage level (NVL) (kV)	BNIR (kA)	I^{Sc} (kA)			
			Year 1	Year 2	Year 3	Year 4
1	138	30	29.46	28.52	28.15	28.93
2	138	30	29.32	29.44	28.57	29.07
15	230	35	29.74	32.01	29.92	31.37
16	230	35	32.12	34.61	32.16	32.96
18	230	35	33.22	32.61	33.95	33.92
21	230	35	33.15	31.49	34.38	33.73
22	230	35	26.01	22.73	31.11	28.90
23	230	35	27.90	28.20	30.91	31.38

B. Comparative Analysis with Cases 2-4

The optimization results including the total invested lines and number of line switching operations in Cases 2-4 are shown in Tables V and VI, respectively. All three cases add 14 new lines during the four-year planning period. Additionally, both Cases 3 and 4 maintain five lines offline each year through switching operations to meet the SCCs. Since the operating cost of wind turbine generators is much lower than that of synchronous generators, all candidate wind turbine generators in the four cases are fully invested in the first year. Hence, the subsequent analysis of GEP primarily focuses on the differences among synchronous generators. Case 1 will be compared with Cases 2-4 to verify the effectiveness of the proposed method, analyzing the impacts of SCCs and GEP on the TEP and system operating cost under a deregulated environment.

TABLE V
TOTAL INVESTED LINES IN CASES 2-4

Case	Total invested lines
Case 2	9-11, 10-11, 10-12, 11-13, 11-14, 11-20, 12-13, 12-22, 14-16, 16-17, 18-19, 19-21, 20-22, 20-23
Case 3	3-24, 9-11, 10-12, 11-13, 11-20, 12-13, 12-22, 14-16, 15-21, 15-24, 16-17, 18-19, 20-22, 20-23
Case 4	1-5, 3-24, 9-12, 10-12, 11-13, 12-22, 12-23, 14-16, 15-21, 15-24, 16-17, 19-20, 20-22, 20-23

TABLE VI
NUMBER OF LINE SWITCHING OPERATIONS IN CASES 2-4

Period	Number of switched-on lines			Number of switched-off lines		
	Case 2	Case 3	Case 4	Case 2	Case 3	Case 4
Year 1	0	0	0	0	0	5
Year 2	0	0	3	0	5	3
Year 3	0	4	3	0	4	3
Year 4	0	3	2	0	3	2

Table VII compare the system short-circuit levels of Cases 1-3 in year 4 with $\Delta I^{Sc(l)} \leq 5$ kA in Case 1, and the fault current I_{sc} is shown in Fig. 4. Case 2 exhibits the short-circuit-level violations at buses 11, 16, 18, and 21, all receiving new transmission lines. Bus 11 shows the most significant

current increase due to its five new transmission lines, signifying the highest expansion among these buses. While in Cases 1 and 3, which consider the SCCs in TEP, no short-circuit-level violations are shown after the investment of new transmission lines. Therefore, it is highly effective and necessary to consider the SCCs in TEP. Since Case 2 does not consider SCCs, its transmission line investment cost is 307 k\$ lower than that in Case 1. This indicates that Case 1 utilizes an additional 8.59% of the investment cost to prevent short-circuit level violations compared with Case 2.

TABLE VII
SHORT-CIRCUIT LEVELS OF CASES 1-3 IN YEAR 4

Bus No.	BNIR (kA)	I^{Sc} (kA)			
		Case 1	Case 2	Case 3 (before GEP)	Case 3 (after GEP)
1	30	28.93	30.49	29.69	29.83
2	30	29.07	30.61	29.77	29.91
11	35	33.52	37.29	24.12	25.48
16	35	32.96	39.34	34.51	36.19
18	35	33.92	36.45	33.82	39.51
20	35	30.29	38.70	34.00	34.69
21	35	33.73	37.87	34.83	39.66
22	35	28.90	31.27	30.34	35.65

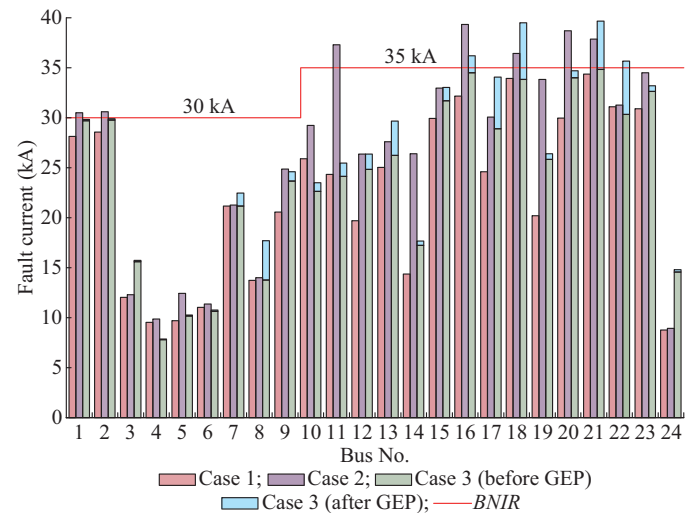


Fig. 4. I^{Sc} of Cases 1-3 in year 4.

As shown in Table VII and Fig. 4, Case 3 does not exhibit any short-circuit-level violations before the GEP. Due to the lack of consideration of the potential impact of GEP on the short-circuit level, Case 3 has a lower investment redundancy compared with Case 1. Its transmission line investment cost is 5.85% lower than that in Case 1. However, there is a certain increase in the short-circuit level at each bus after the GEP. The largest increase occurs at bus 18, where the short-circuit level rises by 5.69 kA. Buses 16, 18, 21, and 22 experience short-circuit-level violations, with exceeding ratios being 3.40%, 12.89%, 13.32%, and 1.86%, respectively. The largest increase occurs at bus 22, with a 17.49% increase.

Figure 5 shows the short-circuit levels of buses with $I^{\text{sc}} \geq 25$ kA in Cases 1 and 3 over the four years, highlighting a significant increase at buses 17, 18, 21, and 22 in Case 3 following GEP investment. Furthermore, Case 3 yields higher annual operating costs than Case 1 due to the exclusion of GEP investment. The above results indicate that neglecting the impact of GEP on TEP could lead to a maximum increase of 17.49% at short-circuit level caused by new GEP investment, along with a maximum 0.50% increase in the system operating cost.

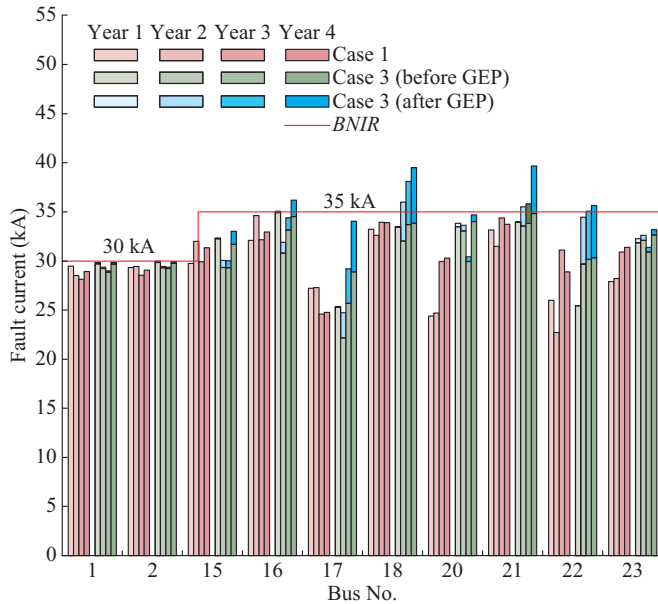


Fig. 5. Short-circuit levels of buses with $I^{\text{sc}} \geq 25$ kA in Cases 1 and 3.

In Table VIII, the system operating cost in Case 4 is superior to that in Case 1, with the maximum difference reaching 3.68%. However, the transmission line investment cost in Case 1 is 10.24% lower than that in Case 4. This is due to the introduction of additional lines in Case 4 to reduce the system operating cost in the objective function, resulting in the lower system operating cost but significantly the higher transmission line investment cost compared with Case 1. Additionally, the investment in synchronous generators for both Cases 1 and 3 requires a significant increase in the LMPs at the respective buses from Fig. 6.

TABLE VIII
SYSTEM OPERATING COSTS OF CASES 1-4

Case	Transmission line investment cost (M\$)	System operating cost of a year (M\$)			
		Year 1	Year 2	Year 3	Year 4
Case 1	3573	577427	625672	685036	730177
Case 2	3266	583902	632439	688339	735589
Case 3	3364	578068	626043	688437	733631
Case 4	3939	556153	614360	675683	731148

However, the generation expansion in Case 4 is not driven by the maximization of generation profits but contributes to the minimization of system operating cost. Thus, the genera-

tion expansion at bus 22 is loss-making in Case 4, and bus 18 in Case 4 has high LMPs but no generator investment. If GEP is based on maximizing the profit of the entity, the new generator would be built at bus 18 instead of bus 22, as shown in Table IX. In contrast, the expansion results for transmission lines and generators in Case 1 are closer to the optimal behavior of each decision-maker under a deregulated environment. There is a certain gap in system operating costs between Cases 1 and 4. However, Case 1 considers the decision of generation expansion under a deregulated environment and obtains the optimal transmission expansion results without exceeding the short-circuit level, in contrast to Cases 3 and 4.

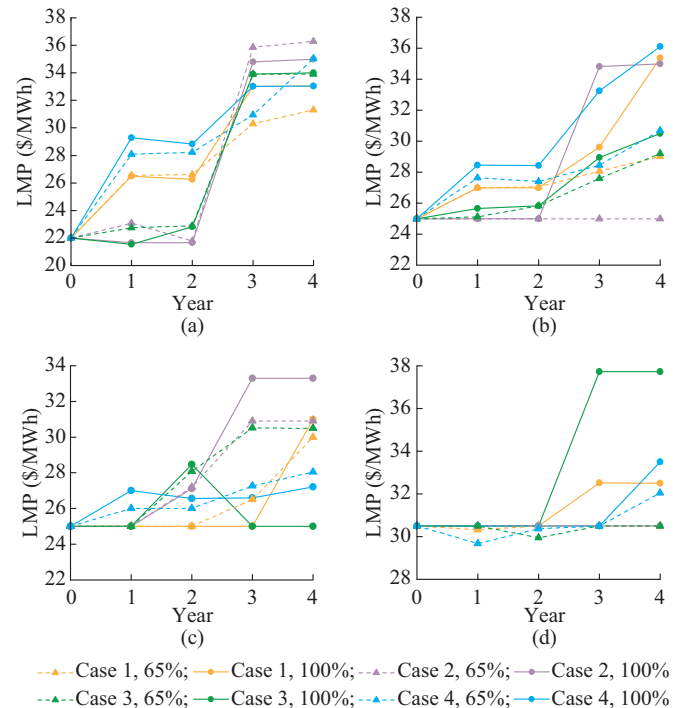


Fig. 6. LMPs of buses 17, 18, 22, and 23 in different cases with 100% and 65% load levels. (a) Bus 17. (b) Bus 18. (c) Bus 22. (d) Bus 23.

TABLE IX
BUSES OF INVESTED GENERATORS IN CASE 4 USING CENTRALIZED METHOD AND UNDER DEREGULATED ENVIRONMENT

Type	Bus (period)	
	Centralized method	Deregulated environment
Synchronous generator	8, 13, 17, 22 (year 1), 23 (year 4)	8, 13, 17, 18 (year 1), 23 (year 4)
Wind turbine generator	16, 21, 22, 23 (year 1)	16, 21, 22, 23 (year 1)

VI. CONCLUSION

This paper proposes a multi-period co-optimization method of transmission and wind turbine GEP with SCCs under a deregulated environment. The proposed method is formulated as a tri-level MILP problem, with the second and third levels restructured into an EPEC problem using the KKT optimality conditions and single-level equivalent with bilinear terms. This problem is restructured into an MILP-NE via CPR. To solve this problem, an iterative algorithm is em-

ployed. Finally, the effectiveness of the proposed method is verified using the modified IEEE 24-bus RTS. The following conclusions are drawn.

1) In comparison to the method excluding SCCs, the proposed method achieves a maximum reduction of 27.78% in the short-circuit level with an additional 8.59% of investment cost, ensuring no exceedance.

2) In comparison to the method without considering the influence of GEP under a deregulated environment, the proposed method incurs a maximum increase in system operating cost of 0.50% while mitigating the 17.49% rise at short-circuit level caused by the newly invested generators.

3) In comparison to the centralized method, the proposed method is more in line with the behavior strategy of independent decision-makers under a deregulated environment, with a 10.24% reduction in transmission line investment cost by avoiding excessive line expansions aimed solely at reducing system operating cost. Additionally, it eliminates the expansion of non-profitable generators by aiming to maximize profits for the generation company.

The next step will focus on expanding research related to the safety standards for power system planning. Verification needs such as system security criteria ($N-1$) and system stability will be addressed by using system simulation tools such as PSD-BPA. The configuration of SFCLs and other current-limiting devices may be further considered in future research for joint planning with system topology.

REFERENCES

- [1] M. Mahdavi, C. Sabillon-Antunez, M. Ajalli *et al.*, "Transmission expansion planning: literature review and classification," *IEEE Systems Journal*, vol. 13, no. 3, pp. 3129-3140, Sept. 2019.
- [2] I.-C. Gonzalez-Romero, S. Wogrin, and T. Gomez, "Review on generation and transmission expansion co-planning models under a market environment," *IET Generation, Transmission & Distribution*, vol. 14, no. 6, pp. 931-944, Mar. 2020.
- [3] J. E. Chillogalli, S. P. Torres, R. R. Romero *et al.*, "Generation and transmission network expansion co-planning models: a comprehensive review," in *Proceedings of 2024 IEEE PES General Meeting*, Seattle, USA, Jul. 2024, pp. 1-5.
- [4] B. Chen and L. Wang, "Robust transmission planning under uncertain generation investment and retirement," *IEEE Transactions on Power Systems*, vol. 31, no. 6, pp. 5144-5152, Nov. 2016.
- [5] M. Taherkhani, S. H. Hosseini, M. S. Javadi *et al.*, "Scenario-based probabilistic multi-stage optimization for transmission expansion planning incorporating wind generation integration," *Electric Power Systems Research*, vol. 189, p. 106601, Dec. 2020.
- [6] H. Jiang, E. Du, N. Zhang *et al.*, "Renewable electric energy system planning considering seasonal electricity imbalance risk," *IEEE Transactions on Power Systems*, vol. 38, no. 6, pp. 5432-5444, Nov. 2023.
- [7] B. Chen, T. Liu, X. Liu *et al.*, "Distributionally robust coordinated expansion planning for generation, transmission, and demand side resources considering the benefits of concentrating solar power plants," *IEEE Transactions on Power Systems*, vol. 38, no. 2, pp. 1205-1218, Mar. 2023.
- [8] J. Li, Z. Li, F. Liu *et al.*, "Robust coordinated transmission and generation expansion planning considering ramping requirements and construction periods," *IEEE Transactions on Power Systems*, vol. 33, no. 1, pp. 268-280, Jan. 2018.
- [9] H. Haghighat and B. Zeng, "Security-constrained robust dynamic power system planning with discrete recourse," *Electric Power Systems Research*, vol. 214, p. 108858, Jan. 2023.
- [10] A. Garcia-Cerezo, R. Garcia-Bertrand, and L. Baringo, "Priority chronological time-period clustering for generation and transmission expansion planning problems with long-term dynamics," *IEEE Transactions on Power Systems*, vol. 37, no. 6, pp. 4325-4339, Nov. 2022.
- [11] A. Garcia-Cerezo, R. Garcia-Bertrand, and L. Baringo, "Enhanced representative time periods for transmission expansion planning problems," *IEEE Transactions on Power Systems*, vol. 36, no. 4, pp. 3802-3805, Jul. 2021.
- [12] A. Moreira, D. Pozo, A. Street *et al.*, "Reliable renewable generation and transmission expansion planning: co-optimizing system's resources for meeting renewable targets," *IEEE Transactions on Power Systems*, vol. 32, no. 4, pp. 3246-3257, Jul. 2017.
- [13] L. C. da Costa, F. S. Thome, J. D. Garcia *et al.*, "Reliability-constrained power system expansion planning: a stochastic risk-averse optimization approach," *IEEE Transactions on Power Systems*, vol. 36, no. 1, pp. 97-106, Jan. 2021.
- [14] F. Moinian and M. T. Ameli, "A reliability-based approach for integrated generation and transmission maintenance coordination in restructured power systems," *Electric Power Systems Research*, vol. 206, p. 107737, May 2022.
- [15] H. Ranjbar, S. H. Hosseini, and H. Zareipour, "Resiliency-oriented planning of transmission systems and distributed energy resources," *IEEE Transactions on Power Systems*, vol. 36, no. 5, pp. 4114-4125, Sep. 2021.
- [16] A. Z. G. Seyyedi, S. M. Rashid, E. Akbari *et al.*, "Co-planning of generation and transmission expansion planning for network resiliency improvement against extreme weather conditions and uncertainty of resiliency sources," *IET Generation, Transmission & Distribution*, vol. 16, no. 23, pp. 4830-4845, Dec. 2022.
- [17] A. Garcia-Cerezo, R. Garcia-Bertrand, and L. Baringo, "Computational performance enhancement strategies for risk-averse two-stage stochastic generation and transmission network expansion planning," *IEEE Transactions on Power Systems*, vol. 39, no. 1, pp. 273-286, Jan. 2024.
- [18] O. H. Abdalla, H. Al-Riyami, A. Al-Busaidi *et al.*, "Review of transmission system security standard in Oman," in *Proceedings of the 12th GCC CIGRE International Conference and 21st Exhibition for Electrical Equipment*, Doha, Qatar, Nov. 2016, pp. 371-380.
- [19] M. Esmaili, M. Ghamsari-Yazdel, N. Amjady *et al.*, "Short-circuit constrained power system expansion planning considering bundling and voltage levels of lines," *IEEE Transactions on Power Systems*, vol. 35, no. 1, pp. 584-593, Jan. 2020.
- [20] M. Esmaili, M. Ghamsari-Yazdel, N. Amjady *et al.*, "Transmission expansion planning including TCSCs and SFCLs: a MINLP approach," *IEEE Transactions on Power Systems*, vol. 35, no. 6, pp. 4396-4407, Nov. 2020.
- [21] G.-H. Moon, J. Lee, and S.-K. Joo, "Integrated generation capacity and transmission network expansion planning with superconducting fault current limiter (SFCL)," *IEEE Transactions on Applied Superconductivity*, vol. 23, no. 3, p. 5000510, Jun. 2013.
- [22] G. Didier, J. Leveque, and A. Rezzoug, "A novel approach to determine the optimal location of SFCL in electric power grid to improve power system stability," *IEEE Transactions on Power Systems*, vol. 28, no. 2, pp. 978-984, May 2013.
- [23] S. Teimourzadeh and F. Aminifar, "MILP formulation for transmission expansion planning with short-circuit level constraints," *IEEE Transactions on Power Systems*, vol. 31, no. 4, pp. 3109-3118, Jul. 2016.
- [24] P. A. A. Panji, A. H. Raditya, and T. Indrawan, "Short-circuit level calculation application for A.C 3 phase on marine and mobile offshore installations based on IEC-61363 standard," *Procedia Engineering*, vol. 194, pp. 545-552, Sept. 2017.
- [25] T. N. Boutsika and S. A. Papatthanassiou, "Short-circuit calculations in networks with distributed generation," *Electric Power Systems Research*, vol. 78, no. 7, pp. 1181-1191, Jul. 2008.
- [26] H. Yao, Y. Xiang, and J. Liu, "Virtual prosumers' P2P transaction based distribution network expansion planning," *IEEE Transactions on Power Systems*, vol. 39, no. 1, pp. 1044-1057, Jan. 2024.
- [27] M. Karimi, M. Kheradnandi, and A. Pirayesh, "Risk-constrained transmission investing of generation companies," *IEEE Transactions on Power Systems*, vol. 34, no. 2, pp. 1043-1053, Mar. 2019.
- [28] J. Wang, H. Zhong, W. Tang *et al.*, "Tri-level expansion planning for transmission networks and distributed energy resources considering transmission cost allocation," *IEEE Transactions on Sustainable Energy*, vol. 9, no. 4, pp. 1844-1856, Oct. 2018.
- [29] Y. Qu, Y. Xiao, X. Wang *et al.*, "An economic incentive mechanism for resilient hardening and expansion based on the Nash bargaining theory," *IEEE Transactions on Power Systems*, vol. 39, no. 3, pp. 5244-5258, May 2024.
- [30] S. Jin and S. M. Ryan, "A tri-level model of centralized transmission and decentralized generation expansion planning for an electricity market - part I," *IEEE Transactions on Power Systems*, vol. 29, no. 1, pp. 132-141, Jan. 2014.

- [31] A. V. Ramesh and X. Li, "Feasibility layer aided machine learning approach for day-ahead operations," *IEEE Transactions on Power Systems*, vol. 39, no. 1, pp. 1582-1593, Jan. 2024.
- [32] R. Fernandez-Blanco, J. M. Arroyo, and N. Alguacil, "On the solution of revenue- and network-constrained day-ahead market clearing under marginal pricing – part I: an exact bilevel programming approach," *IEEE Transactions on Power Systems*, vol. 32, no. 1, pp. 208-219, Jan. 2017.
- [33] R. Walling, R. Harley, D. Miller *et al.*, "Fault current contributions from wind plants," in *Proceedings of 2015 68th Annual Conference for Protective Relay Engineers*, New York, USA, Apr. 2015, pp. 137-227.
- [34] L. Strezoski, M. Prica, and K. A. Loparo, "Generalized Δ -circuit concept for integration of distributed generators in online short-circuit calculations," *IEEE Transactions on Power Systems*, vol. 32, no. 4, pp. 3237-3245, Jul. 2017.
- [35] H. A. Al-Riyami, A. A. Busaidi, A. Al-Nadabi *et al.*, "Grid code compliance for integrating 50 MW wind farm into dhofar power grid," in *Proceedings of 12th GCC-CIGRE International Conference and 21st Exhibition for Electrical Equipment*, Doha, Qatar, Aug. 2016, pp. 152-161.
- [36] Probability Methods Subcommittee, "IEEE reliability test system," *IEEE Transactions on Power Apparatus and Systems*, vol. 98, no. 6, pp. 2047-2054, Dec. 1979.

Zhaoqin Hu received the B.S. degree in electrical engineering from Xi'an Jiaotong University, Xi'an, China, in 2023. He is currently working toward

the M.S. degree in electrical engineering with Xi'an Jiaotong University, Xi'an, China. His research interests include electricity market and power system optimization.

Yunpeng Xiao received the B.S. and Ph.D. degrees in electrical engineering from Xi'an Jiaotong University, Xi'an, China, in 2012 and 2018, respectively. From 2016 to 2017, he was a Visiting Ph.D. student with the Technical University of Denmark, Lyngby, Denmark. He is currently an Associate Professor with the School of Electrical Engineering, Xi'an Jiaotong University. His research interests include electricity market towards renewable energy and entity interaction in Energy Internet.

Xiuli Wang received the B.S., M.S., and Ph.D. degrees in electrical engineering from Xi'an Jiaotong University, Xi'an, China, in 1982, 1985, and 1997, respectively. She is currently a Professor with the School of Electrical Engineering, Xi'an Jiaotong University. Her research interests include power system planning, integration of renewable energy, electricity market, and novel transmission scheme.

Xifan Wang received the B. S. degree from Xi'an Jiaotong University, Xi'an, China, in 1957. From 1983 to 1986, he was a Visiting Scientist with Cornell University, Ithaca, USA. From 1991 to 1994, he was a Visiting Professor with the Kyushu Institute of Technology, Kitakyushu, Japan. He is an Academician of the Chinese Academy of Science and a Professor with the School of Electrical Engineering, Xi'an Jiaotong University. His research interests include power system analysis, operation, and planning, and novel transmission scheme.